Third-Order Elastic Moduli of Strontium Fluoride†

S. ALTEROVITZ AND D. GERLICH
Department of Physics and Astronomy, Tel Aviv University, Ramat Aviv, Israel
(Received 16 June 1969)

The complete set of the second- and third-order elastic moduli of single-crystal strontium fluoride was determined from measurements of sound velocity and its changes under uniaxial and hydrostatic compression at room temperature. The values of the measured third-order elastic moduli in units of 10^{11} dyn/cm^2 are $C_{111}=-82.1$, $C_{112}=-30.9$, $C_{144}=-9.5$, $C_{166}=-17.5$, $C_{123}=-18.1$, and $C_{456}=-4.2$. The experimentally measured third-order elastic moduli were compared with the theoretically calculated ones, and agreement was found. Conclusions pertaining to the lattice forces interactions in strontium fluoride are presented. The measured values of the third-order elastic moduli are correlated with the thermal expansion.

INTRODUCTION

SEVERAL studies of the third-order elastic moduli (TOEM) of the alkaline-earth fluorides have been published during recent years.[1–5] These materials are interesting from the aspect of their lattice dynamics, having the fluorite structure, viz., not every atom in the lattice is a center of symmetry. Thus, the possibility of relative motion of the different sublattices under strain arises, and even in the case of central forces interactions only, the Cauchy relations may be violated. As the complete set of the TOEM for CaF_2 and BaF_2 has previously been reported, it seems to be of interest to carry out similar measurements on other members of the group of alkaline-earth fluorides. With this in mind the present work was undertaken. It reports measurements of the second-order elastic moduli (SOEM) around room temperature and of the TOEM at room temperature. The experimentally measured TOEM are compared with theoretically computed values, and some conclusions pertaining to the atomic forces in the SrF_2 lattice presented.

EXPERIMENTAL

The samples used in the present work were single crystals of SrF_2 purchased from Optovac Inc. The crystals were cube shaped, sizes 16×17×20 mm approximately, their faces corresponding to the (110), (1$\bar{1}$0), and (001) crystalline planes. The crystals were hand lapped until the faces were parallel within a few parts in 10^5, and then the orientation of the faces was checked by x-ray Laue backreflection. The faces were found to correspond to the crystalline planes within $\frac{1}{2}°$.

Strontium fluoride, being cubic, has three independent SOEM (C_{11}, C_{12}, and C_{44}) and six independent TOEM (C_{111}, C_{112}, C_{144}, C_{166}, C_{123}, and C_{456}), Brugger's definitions[6] for the TOEM being used throughout. The SOEM were determined from the absolute value of the sound velocity, while the changes in this velocity under uniaxial and hydrostatic compression yield the TOEM. With the available samples, five different sound-propagation modes were available for the determination of the SOEM, while 14 different combinations of propagation modes and pressure direction[7] were available for determining the TOEM. Both sets of moduli were then computed by a least-square fit.

The sound waves were generated by means of X- and Y-cut crystalline quartz transducers, operating at their fundamental frequency of 15 MHz. The transducers were bonded to the samples with phenylsalicylate (salol).

In order to prevent the cracking of the samples during the uniaxial compression, and to eliminate dislocation-line movement which might falsify completely the results,[8,9] the stress level was kept very low, never exceeding 15 kg/cm^2. Also, the samples were irradiated with an x-ray dose of 5000 R prior to the start of the measurements. Such irradiation creates additional pinning centers for the dislocation lines, thus preventing their motion.[10]

The absolute value of the sound velocity was determined by the McSkimin pulse-superposition method,[11,12] the changes in the sound velocity, by the frequency-modulated pulse-superposition method.[13,14] The temperature of the sample being investigated was monitored carefully all the time, and all results were normalized to 295°K.

The absolute value of the sound velocity was determined from the round-trip travel time t. The latter was deduced from the following equation[11]:

$$T=pt-p\beta/360f+n/f. \quad (1)$$

† Based on a thesis submitted by S. Alterovitz to the Tel Aviv University in partial fulfilment of the requirements for a Ph.D. degree.

[1] P. S. Ho and A. L. Ruoff, Phys. Rev. **161**, 864 (1967).
[2] C. Wong and D. E. Schuele, J. Phys. Chem. Solids **28**, 1225 (1968).
[3] D. Gerlich, Phys. Rev. **168**, 947 (1968).
[4] C. Wong and D. E. Schuele, J. Phys. Chem. Solids **29**, 1309 (1968).
[5] S. Alterovitz and D. Gerlich, Phys. Rev. **184**, 999 (1969).
[6] K. Brugger, Phys. Rev. **133**, A1611 (1964).
[7] R. N. Thurston and K. Brugger, Phys. Rev. **133**, A1604 (1964).
[8] Y. Hiki and A. V. Granato, Phys. Rev. **144**, 411 (1966).
[9] K. Salama and G. A. Alers, Phys. Rev. **161**, 673 (1967).
[10] R. Gordon and A. S. Nowick, Acta Met. **4**, 514 (1956).
[11] H. J. McSkimin, J. Acoust. Soc. Am. **33**, 12 (1961).
[12] H. J. McSkimin and P. Andreatch, Jr., J. Acoust. Soc. Am. **34**, 609 (1962).
[13] H. J. McSkimin, J. Acoust. Soc. Am. **37**, 864 (1965).
[14] H. J. McSkimin and P. Andreatch, Jr., J. Acoust. Soc. Am. **41**, 1052 (1967).

TABLE I. Round-trip travel time of the sound for different propagation modes in SrF_2.

Mode No.	Propagation direction	Polarization direction	Length (cm)	Transit time (μsec)	ρv^2 (10^{11} dyn/cm^2)
1	[110]	[110]	1.6506±0.0001	6.326±0.002	11.650±0.007
2	[001]	[001]	2.0414±0.0001	7.564±0.002	12.463±0.005
3	[110]	[1$\bar{1}$0]	1.6506±0.0001	10.802±0.002	3.996±0.002
4	[110]	[001]	1.6506±0.0001	12.090±0.002	3.190±0.001
5	[001]	(001) plane	2.0414±0.0001	4.958±0.002	3.187±0.001

TABLE II. SOEM of SrF_2 at 295°K. (Units are 10^{11} dyn/cm^2.)

	C_{11}	C_{12}	C_{44}	B^S
Present results	12.461±0.005	4.463±0.011	3.1874±0.0010	7.130±0.009
Gerlich[a]	12.36	4.314	3.132	6.996

[a] Reference 15.

Here, T is the measured inverse resonant frequency, $p=2$, f is the sound wave frequency, and β is the phase angle associated with the reflection of the sound wave at the transducer and bond. The angle β was calculated as a function of the frequency around 15 MHz, utilizing the mechanical impedances of the sample, bond, and transducer. The calculation was performed assuming no phase shift in the bond ($\tan B_1 l_1=0$), which is well obeyed for salol bonds. (Their $B_1 l_1$ values are up to 1°.) The resonant frequency corresponding to $n=0$ was deduced by carrying out three sets of measurements of T for every propagation mode. The first two were for $p=2$ and $p=3$ at different values of n and a fixed frequency f. The third one was for $p=2$ at different values of n, but at a frequency of $0.9f$. From these three sets of measurements and the computed values of the β's, the time t was found. The accuracy obtained was better than one part in 10^4.

The uniaxial stress was generated by means of a manually operated home-made press, and measured by a factory-calibrated load cell. Lead shims were placed

TABLE III. Material parameters for SrF_2 at 295°K.

X-ray density[a]	4.278 gm/cm^3
Specific heat at constant pressure[b]	69.8 J/mole deg
Coefficient of linear thermal expansion[b]	1.82×10^{-5} deg^{-1}
Isothermal bulk modulus	6.946×10^{11} dyn/cm^2

[a] Reference 15.
[b] Reference 16.

TABLE IV. Values of $(\rho_0 W^2)'_{P=0}$ for the different propagation modes.

Mode No.	Propagation direction	Polarization direction	Stress direction	$(\rho_0 W^2)'_{P=0}$
1	[110]	[110]	[001]	0.735 ±0.033
2	[1$\bar{1}$0]	[110]	[001]	0.0693±0.0066
3	[110]	[001]	[001]	0.453 ±0.003
4	[001]	[001]	[1$\bar{1}$0]	0.950 ±0.028
5	[001]	[110]	[110]	0.540 ±0.006
6	[001]	[1$\bar{1}$0]	[110]	0.172 ±0.013
7	[110]	[110]	[1$\bar{1}$0]	−0.780 ±0.036
8	[1$\bar{1}$0]	[110]	[110]	−0.0929±0.007
9	[110]	[001]	[1$\bar{1}$0]	0.0949±0.0024
10	[001]	[110]	Hydrostatic	0.9328±0.0022
11	[110]	[110]	Hydrostatic	5.317 ±0.012
12	[110]	[1$\bar{1}$0]	Hydrostatic	0.1200±0.0006
13	[001]	[001]	Hydrostatic	4.687 ±0.008
14	[110]	[001]	Hydrostatic	0.9409±0.0014

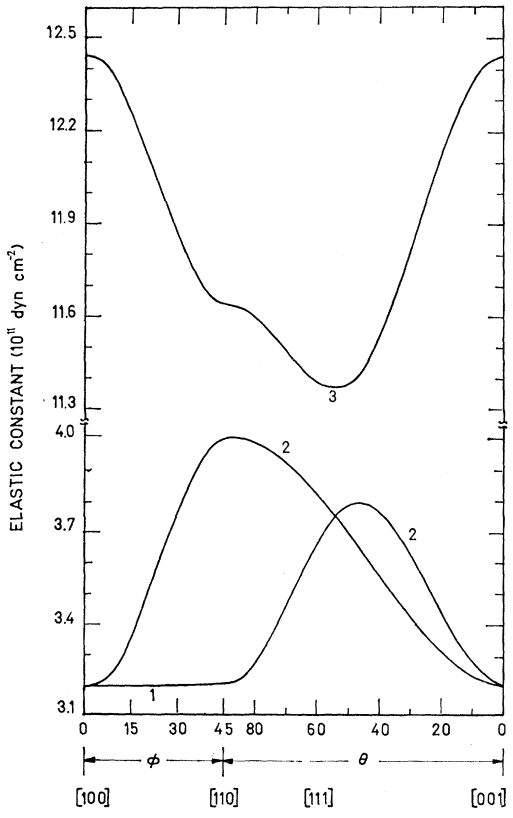

FIG. 1. Values of ρv^2 for some directions of high symmetry.

TABLE V. TOEM for SrF_2 at 295°K. (Units are 10^{11} dyn/cm².)

C_{111}	C_{112}	C_{123}	C_{144}	C_{166}	C_{456}
−82.1±1.1	−30.9±0.5	−18.1±1.2	−9.51±0.66	−17.5±0.3	−4.21±0.28

between the sample and the pressurizing surfaces in order to prevent the application of shear stresses to the sample. The hydrostatic compression was generated by a nitrogen-gas compressor, and measured with a Bourdon gauge.

RESULTS

Table I presents the values of the round-trip travel time t for the five different modes in our crystals. From the latter data, the three SOEM are calculated by a least-squares fit and are shown in Table II. The results agree very well with earlier ones.[15] From the SOEM, the value of ρv^2 in any direction may be calculated, where ρ is the density, and v is the sound velocity. The values of ρv^2 for some directions of high symmetry are shown in Fig. 1. Here 3 refers to the longitudinal mode, 1 and 2 refer to the slow and fast shear modes, respectively. Figure 1 bears out the elastic anisotropy of SrF_2. The material parameters of SrF_2, required in the computation of the SOEM and TOEM are shown in Table III.[16]

The changes in the sound velocity under hydrostatic and uniaxial compression are summarized in Table IV and Figs. 2–4. The graphs represent the measured reciprocal resonant frequency for the 14 different combinations of propagation and stress direction as a function of the applied stress. The straight lines are the least-squares fit to the experimental data. From the slopes of these lines, the pressure derivatives at zero pressure of $\rho_0 W^2$, viz., $(\rho_0 W^2)'_{P=0}$, are determined. Here, ρ_0 is the zero-pressure density, W is the "natural" velocity. The values of $(\rho_0 W^2)'_{P=0}$ are presented in Table IV. As can be seen from the graphs, the changes in sound velocity are linear up to the highest applied uniaxial stress, which is a necessary condition (but not sufficient[9]), that no dislocation-lines motion has occurred. From the values of $(\rho_0 W^2)'_{P=0}$ the six TOEM are computed, the results being shown in Table V. From

TABLE VI. Pressure derivatives of the effective SOEM (ρv^2) of SrF_2 at 295°K.

$(\partial C_{11}/\partial P)_T$	$(\partial C_{12}/\partial P)_T$	$(\partial C_{44}/\partial P)_T$
5.25±0.04	4.52±0.07	1.07±0.03

TABLE VII. Temperature dependence of the sound travel time for the different propagation modes.

Mode No.	Propagation direction	Polarization direction	ρv^2	$d\ln t/dT$ (10^{-6} deg^{-1})
1	[110]	[110]	C_L	108.36
2	[001]	[001]	C_{11}	85.83
3	[110]	[1$\bar{1}$0]	C'	63.44
4	[110]	[001]	C_{44}	134.75
5	[001]	(001) plane	C_{44}	134.24

TABLE VIII. Temperature derivatives of the SOEM of SrF_2 at 295°K. (Units are 10^{-4} deg^{-1}.)

	$(\partial \ln C_{11}/\partial T)_p$	$(\partial \ln C_{12}/\partial T)_p$	$(\partial \ln C_{44}/\partial T)_p$
Present results	−1.915±0.006	−2.79±0.03	−2.90±0.02
Gerlich[a]	−1.6 ±0.16	−3.8 ±0.4	−2.7 ±0.3

[a] Reference 15.

TABLE IX. Comparison of uniaxial and hydrostatic data. (Units are 10^{11} dyn/cm².)

	$C_{111}+2C_{112}$	$C_{144}+2C_{166}$	$C_{111}-C_{123}$
Hydrostatic	−143.4±0.8	−46.5±0.6	−65.1±1.7
Uniaxial	−161.6±9.8	−45.7±2.1	−69.7±7.3

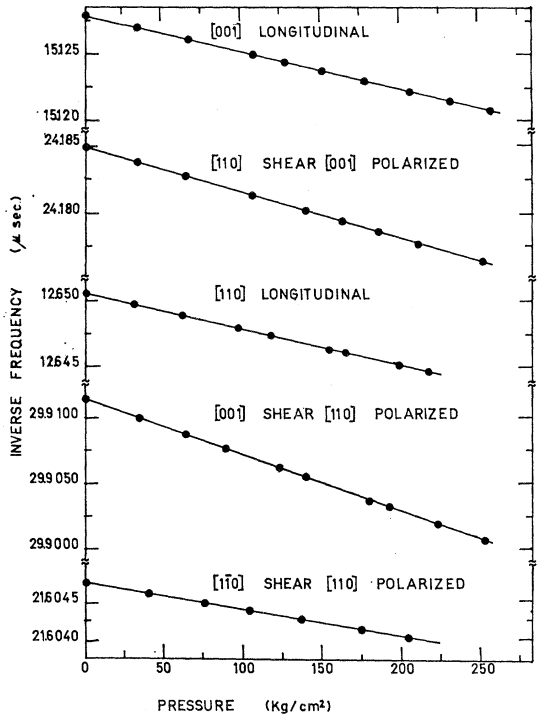

FIG. 2. Reciprocal resonant frequency as a function of hydrostatic pressure for different propagation modes.

[15] D. Gerlich, Phys. Rev. **136**, A1366 (1964).

[16] A. C. Bailey and B. Yates, Proc. Phys. Soc. (London) **91**, 390 (1967).

TABLE X. Comparison of the experimental and theoretical values of the TOEM of SrF_2. (Units are 10^{11} dyn/cm^2. nn: nearest-neighbor interaction; nnn: next-nearest-neighbor interaction.)

	C_{111}	C_{112}	C_{123}	C_{144}	C_{166}	C_{456}
Experimental	−82.1	−30.9	−18.1	−9.5	−17.5	−4.2
Rigid-ion model, nn and nnn	−68.5	−36.5	−23.6	−12.8	−22.2	−5.2
Shell-model, nn and nnn	−68.5	−36.5	−23.6	−9.8	−20.1	−6.2
Rigid-ion model, nn only	−62.2	−37.1	−24.2	−11.2	−19.5	−2.3

the hydrostatic data alone, the pressure derivatives of the effective SOEM, viz., $(\rho v^2)'_{P=0}$, may be calculated by a least-square fit, and are shown in Table VI.

In order to normalize all measurements to 295°K, the temperature derivatives of the SOEM are required. They were determined from the temperature variation of t over the temperature range 273–300°K. In this range the changes were found to be linear, the results being shown in Table VII. From the five experimentally measured derivatives of the travel time, the three temperature derivatives of the SOEM are computed by a least-square fit, and shown in Table VIII, together with similar data deduced from earlier measurements.[15]

In order to ascertain that no dislocation-lines motion has occurred during uniaxial compression, the uniaxial data alone were utilized to determine the six TOEM. The latter were used to form the three linear combinations which are determined by the hydrostatic runs alone, viz., $C_{111}+2C_{112}$, $C_{144}+2C_{166}$, $C_{111}-C_{123}$, and the latter were then compared with the similar results deduced from the hydrostatic measurements. The comparison is shown in Table IX, and as can be seen, the agreement between the two sets indicates that probably no dislocation-lines motion has occurred.

The errors in the quantities obtained by a least-square fit are the standard deviations multiplied by 0.675. This was found to be the largest error, including all possible sources of error like temperature drift, uncertainties in the measurement of frequency, stress and temperature, and errors in the relative orientation of the propagation direction, polarization, and stress. It was also found that carrying out the least-square fits either with equal weights or with weights equal to the reciprocals of the standard deviations did not change the results materially.

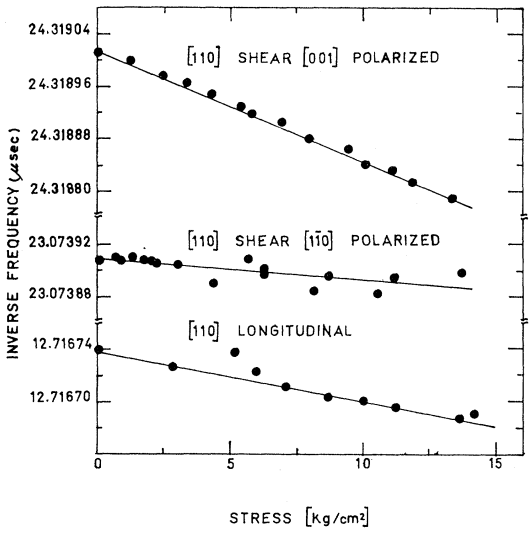

FIG. 3. Reciprocal resonant frequency as a function of uniaxial compression in the [001] direction for different propagation modes.

DISCUSSION

A. Comparison with Theory

Assuming a model of central-forces interaction, consisting of Coulombic interaction throughout the lattice and exchange forces between nearest and next-nearest neighbors, Srinivasan[17] has evaluated theoretically the TOEM for the fluorite structure. In his calculation he had used force parameters taken from a shell-model calculation by Axe,[18] the latter calculation having been done to explain the difference between the measured values of C_{12} and C_{44} for the alkaline-earth fluorides. For his calculation, Axe[18] had used an erroneous shell charge for the cation, as pointed out by Dick,[19] and also neglected the core-core interaction in the evaluation of the shell correction to the rigid-ion model.

We have recalculated the TOEM by Srinivasan's procedure, but using the correct force parameters and taking into account the core-core interaction. The calculation was carried out for three models: (i) rigid-ion model, assuming the spring constant K_2 of the shell-core interaction in fluorine to be infinite, and the shell

TABLE XI. Cauchy relations for SrF_2.

C_{12}/C_{44}	C_{112}/C_{166}	C_{123}/C_{144}	C_{144}/C_{456}
1.401	1.766	1.903	2.259

TABLE XII. Comparison of the values of γ_L and γ_H from elastic and thermal-expansion data.

	γ_L	γ_H
Elastic	0.74	0.95
Thermal expansion	0.74 (30°K)	1.62 (270°K)

[17] R. Srinivasan, Phys. Rev. **165**, 1054 (1968).
[18] J. D. Axe, Phys. Rev. **139**, A1215 (1965).
[19] B. G. Dick, Phys. Rev. **145**, 609 (1966).

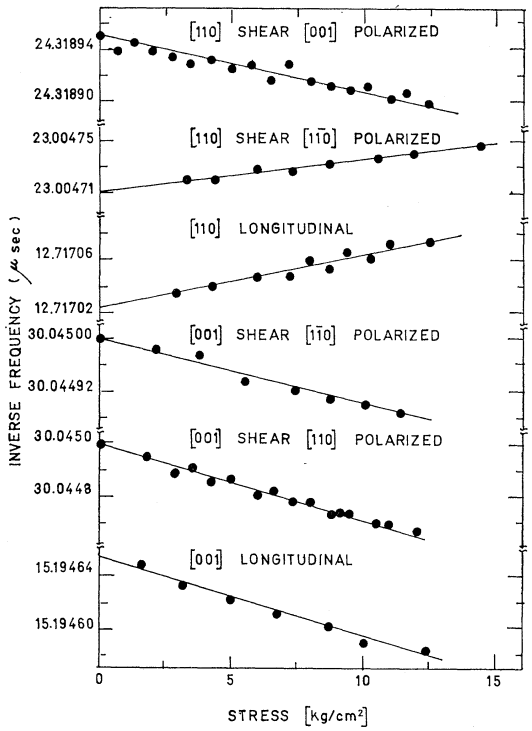

FIG. 4. Reciprocal resonant frequency as a function of uniaxial compression in the [110] direction for different propagation modes.

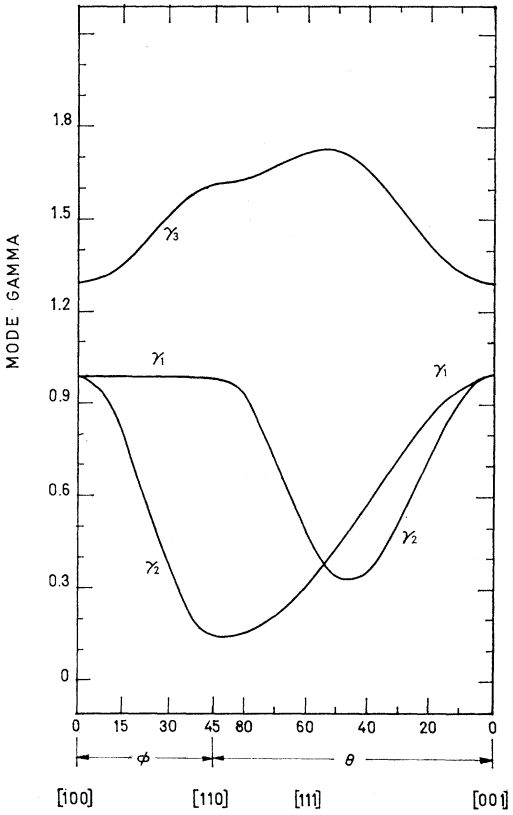

FIG. 5. Mode γ's as a function of crystalline direction.

charge Y_2 to be zero; (ii) shell model, with nearest- and next-nearest neighbor interaction, assuming $k_2=8\times10^5$ dyn/cm and $Y_2=-1.9$; (iii) rigid-ion model, with nearest-neighbor interaction only, which is the simplest model that can be assumed. For all models, the repulsive potential was taken to be of the form Ar^{-n}, where r is the distance between the interacting ions, and A and n are constants. The constant n was in the range 6–12, and is found that varying n from 6 to 12 changed C_{111} by 3% while the remaining TOEM changed even less. In Table X, the three sets of TOEM calculated on the basis of the above models are shown, together with the experimental data. The computation was done assuming $n=9$.

As can be seen from Table X, the agreement between the experimental and theoretical TOEM is quite good, especially bearing in mind that we are concerned with quantities which are measured by a second-order effect, and the simplicity of the model. It should also be pointed out that the theoretical calculation is for 0°K, while our measurements were done at 295°K. However, the change in the TOEM between room temperature and 0°K is believed to be small (less than 10%) for the alkaline-earth fluorides. This is based on the measurements[4] done for CaF_2 and BaF_2 at 298 and 195°K, in which the three combinations of the TOEM obtained from hydrostatic measurements varied by less than 2% over the above temperature range.

It is noteworthy that the rigid-ion model as used here, has only three parameters, C_{11}, C_{12}, and n, and being insensitive to n, is indeed very simple, and yields a surprisingly good agreement between experiment and theory for five out of the six TOEM (except for C_{111}). The reason for such a good agreement is that the Sr-F interaction is much stronger that the F-F (60 times larger), a fact that is obvious from the last row of Table X, where the F-F interaction is neglected. The value of C_{111} is made up of contributions from the second nearest and farther neighbors, and the calculation will therefore yield a value which is smaller than the experimentally measured one. The same situation exists[3,5] in the case of CaF_2 and BaF_2. A similar behavior for C_{111} is also found in the case of alkali halides.[20] Thus, it may be that C_{111} contains contributions from more distant neighbors than other TOEM in all cubic crystals.

The values of the ratios of the SOEM and TOEM which should have been equal to unity were the Cauchy relations obeyed, are shown in Table XI. It is obvious that the Cauchy relations are violated for SrF_2, although the values of the SOEM and TOEM can be explained by a model of central forces interactions only. The reason for this violation must therefore be the relative

[20] P. B. Ghate, Phys. Rev. 139, A1666 (1965).

motion of the sublattices under stress, which is possible in the case of the fluorite structure.

B. Grüneisen γ's

From the values of the SOEM at room temperature and 0°K together with their pressure derivatives (Table VI), the mode Grüneisen γ's $\gamma_i (i=1, 2, 3)$ and the low- and high-temperature limits of their thermal average γ_L and γ_H may be evaluated.[4,21] The γ_i's for some directions of high symmetry are shown in Fig. 5, where ϕ denotes the azimuthal angle, θ denotes the colatitude, γ_3 refers to the longitudinal mode, and γ_1 and γ_2 refer to the slow and fast shear modes, respectively. In Table XII, γ_L and γ_H are shown together with the values deduced from thermal expansion.[16] As can be seen, there is a good agreement between the two sets for γ_L, while the values of γ_H disagree. This is also the case[1–5] for CaF_2 and BaF_2, and is probably due to the contributions of the optical modes to the thermal expansion value of γ_H.

[21] D. E. Schuele and C. S. Smith, J. Phys. Chem. Solids **25**, 801 (1964).

PHYSICAL REVIEW B VOLUME 1, NUMBER 6 15 MARCH 1970

Self-Consistent-Field Approach to Lattice Dynamics*

W. C. KERR AND A. SJÖLANDER†
Argonne National Laboratory, Argonne, Illinois 60439
(Received 2 September 1969)

The self-consistent-field theory of lattice dynamics is examined with particular emphasis on the physical assumptions entering this approach. The solution of the basic equation is generalized beyond that of earlier treatments to include damping and the corresponding frequency shifts of the collective modes. The expressions found for the damping and frequency shifts contain renormalized anharmonic force constants but otherwise are essentially the same as those derived in conventional perturbation theory.

I. INTRODUCTION

A VARIETY of physical problems concerning the dynamics of many-body systems has been treated in a self-consistent-field (SCF) approach. In this method complicated many-body interactions are replaced by some simplifying effective field. The form of this field depends, of course, on the particular system being considered. For example in the random-phase approximation[1] for the high-density electron gas, one introduces the time-dependent self-consistent Hartree potential as the effective potential acting on an electron. In discussing the dynamics of spin systems in the molecular-field approximation,[2] one replaces the interaction between the spins by a self-consistent magnetic field acting on the individual spins. Phase transitions in ferroelectrics[3] and transitions from one lattice structure to another[4] have been handled in a similar self-consistent-field approach.

The traditional theory of lattice dynamics[5] has failed for solid helium because of the large zero-point vibrations,[6] and therefore other approaches have been proposed.[7–13] Brenig[11] was the first to suggest a SCF approach, and this has been further developed by Fredkin and Werthamer (FW)[12] and by Gillis and Werthamer (GW).[13] Because of its mathematical simplicity and its flexibility to incorporate many physical effects, it is particularly interesting to pursue this method.

The aim of this paper is first to reexamine the theory of FW and GW. By solving their basic equation in a different way, we are able to elucidate more clearly the physical assumptions going into this approach. Second we generalize our method of solving their basic equation to include phonon-damping effects.

The outline of this paper is as follows. Section II contains the formulation of the SCF approach. Our method of solving the basic equation of motion is presented in Sec. III. In order to prove that the physical assumption made in Sec. III is identical to the more mathematical assumption of GW, we briefly discuss in Sec. IV their solution of the basic equation of motion.

* Paper based on work performed under the auspices of the U. S. Atomic Energy Commission.
† On leave of absence from the Institute of Theoretical Physics, S-402 20 Göteborg 5, Sweden.
[1] D. Pines and P. Nozières, *The Theory of Quantum Liquids* (W. A. Benjamin, Inc., New York, 1966), Vol. I.
[2] S. V. Tyablikov, *Methods in the Quantum Theory of Magnetism* (Plenum Press, Inc., New York, 1967).
[3] P. B. Miller and P. C. Kwok, Phys. Rev. **175**, 1062 (1968).
[4] N. Boccara and G. Sarma, Physics **1**, 219 (1965).
[5] M. Born and K. Huang, *Dynamical Theory of Crystal Lattices* (Oxford University Press, Oxford, England, 1954).
[6] F. W. de Wette and B. R. A. Nijboer, Phys. Letters **18**, 19 (1965).
[7] T. R. Koehler, Phys. Rev. Letters **18**, 654 (1967).
[8] T. R. Koehler, Phys. Rev. **165**, 942 (1968).
[9] P. Choquard, *The Anharmonic Crystal* (W. A. Benjamin, Inc., New York, 1967).
[10] H. Horner, Z. Physik **205**, 72 (1967).
[11] W. Brenig, Z. Physik **171**, 60 (1963).
[12] D. R. Fredkin and N. R. Werthamer, Phys. Rev. **138**, A1527 (1965). This paper will be referred to as FW.
[13] N. S. Gillis and N. R. Werthamer, Phys. Rev. **167**, 607 (1968); **173**, 918(E) (1968). This paper will be referred to as GW.